

Ordered surface alloy formation of immiscible metals: The case of Pb deposited on Ag(111)J. Dalmas,¹ H. Oughaddou,^{1,*} C. Léandri,¹ J.-M. Gay,¹ G. Le Lay,¹ G. Tréglia,¹ B. Aufray,¹ O. Bunk,² and R. L. Johnson³¹*CRMCN-CNRS, Campus de Luminy, Case 913, 13288 Marseille Cedex 09, France*²*Paul Scherrer Institut, Swiss Light Source / WLG-223, 5232 Villigen PSI, Switzerland*³*Institut für Experimentalphysik, Universität Hamburg, Luruper Chaussee 149, D-22761 Hamburg, Germany*

(Received 2 March 2005; revised manuscript received 1 August 2005; published 20 October 2005)

The deposition of $1/3$ Pb monolayer at room temperature onto Ag(111) leads to a $(\sqrt{3} \times \sqrt{3})R30^\circ$ superstructure. We present here a detailed structural study of this surface structure by synchrotron radiation surface x ray diffraction (SR-SXRD) and scanning tunnel microscopy (STM). We show that Pb atoms are embedded into the silver top surface layer forming an ordered Ag_2Pb surface alloy despite the strong tendency of the system to phase separate in the bulk. Quenched molecular dynamics simulations allow us to interpret this ordering reversal, in terms of size-mismatch induced surface alloying.

DOI: [10.1103/PhysRevB.72.155424](https://doi.org/10.1103/PhysRevB.72.155424)

PACS number(s): 68.55.Jk, 61.82.Bg, 68.37.Ef, 61.10.Nz

I. INTRODUCTION

Metallic thin films deposited on metallic substrates have been the subject of a large number of investigations in relation to possible technological applications. Indeed, the formation of surface alloys which may appear during the growth process can present new chemical and physical properties due to their small thickness (typically a few atomic layers) and their possible peculiar chemical structure. As described in most modern theories,¹⁻⁴ (for a review see Ref. 5), the composition of these surface alloys is closely related to chemical interactions between the elements involved (deposit and substrate), their size mismatch and their relative surface segregation tendencies.¹⁻⁵ When the deposited element has a strong tendency to segregate to the surface of the substrate, the deposition of a single monolayer can lead either to a dense plane generally in pseudo epitaxy above the surface, or to the formation of a two-dimensional (2D) ordered surface alloy in relation with the bulk chemical tendency of both elements, i.e., a tendency to phase separation or to the formation of ordered compounds. This has been experimentally shown on two model systems: Ag/Cu(111) in the former case^{6,7} and Sb/Cu(111) in the latter one.⁸

The Pb/Ag(111) system is quite similar to the Ag/Cu(111) one. Indeed both systems present (i) a strong tendency to phase separation, (ii) a strong surface segregation tendency of the deposited element, and (iii) a size effect which acts in the same sense (deposited atoms are larger than substrate ones) but which is almost twice as large in the present case! It was then tempting to predict a behavior similar to that observed for Ag/Cu(111), namely the formation of pure close-packed Pb islands the sizes of which increase with coverage, up to the formation of a pure Pb(111) monolayer. In this scenario, neither intermixing nor formation of a 2D ordered intermetallic compound is expected. This scenario is partly invalidated at intermediate coverage ($1/3$ Pb monolayer) by previous works using Auger electron spectroscopy (AES) and low energy electron diffraction (LEED)^{9,10} which revealed a $(\sqrt{3} \times \sqrt{3})R30^\circ$ superstructure before the formation of the dense plane, which is also observed during segregation kinetics of lead from a

Ag(Pb)(111) solid solution. Consistently, with the phase separation tendency of the system, this intermediate superstructure has been interpreted, assuming no intermixing, as an ordered array of Pb adatoms adsorbed in threefold positions. More recently, this has been questioned by a STM study which suggests a possible Pb incorporation during the early stages of the deposition.^{11,12}

In this paper we present a complete and detailed atomic structure of this $(\sqrt{3} \times \sqrt{3})R30^\circ$ superstructure using synchrotron radiation surface x ray diffraction (SR-SXRD) and scanning tunnel microscopy (STM). We show that the Pb atoms are indeed embedded into the Ag top layer, thus forming a highly perfect Ag_2Pb surface alloy. This chemical tendency reversal at the surface is then confirmed by a quenched-molecular-dynamics simulation of the adsorption/substitution process within a potential derived from the second-moment approximation (SMA) of the tight binding scheme.

II. EXPERIMENTAL

The sample was prepared at the synchrotron radiation center (HASYLAB) at Desy in Hamburg in an ultrahigh-vacuum system with careful surface preparation using several characterization tools. The Ag(111) substrate was cleaned by repeated cycles of sputtering with Ar^+ ions (500 eV) and annealing at high temperatures (400°C–600°C) until a sharp $p(1 \times 1)$ LEED pattern was obtained. Pb was deposited onto the substrate at room temperature (RT) from a calibrated effusion cell with a pyrolytic boron nitride crucible at a pressure of 2×10^{-10} Torr. The sample is alternately placed in front of the Pb evaporation cell for a given time, then in front of an Auger spectrometer to monitor the surface concentration and then in front of LEED optics to observe the surface structure.

At about $1/3$ Pb ML coverage, a sharp $(\sqrt{3} \times \sqrt{3})R30^\circ$ reconstruction was obtained. Next, the sample was transferred without breaking the vacuum to a portable ultrahigh-vacuum chamber (base pressure less than 10^{-9} Torr), with a hemispherical Be window. The portable chamber was mounted within few minutes on a vertical diffractometer at the BW2 beamline for grazing incidence x ray diffraction

measurements. The x ray wavelength was selected to be 1.239 \AA using a silicon double-crystal monochromator. The angle of incidence was kept fixed at 0.35° during the measurements (slightly larger than the critical angle for total reflection of Ag). The STM measurements were performed separately in Marseille, France in an ultrahigh-vacuum system housing an Omicron-STM.

III. RESULTS AND DISCUSSION

After deposition of $1/3$ Pb ML onto the Ag(111) surface, the LEED observations revealed a sharp $(\sqrt{3} \times \sqrt{3})R30^\circ$ superstructure. A filled-state STM image area of the Pb/Ag(111) surface is displayed in Fig. 1. This image taken at atomic resolution shows a regular array of protrusions which can be associated to Pb atoms in the $(\sqrt{3} \times \sqrt{3})R30^\circ$ superstructure, since they are separated by $\sim 5 \text{ \AA} = a_{\text{Ag}} \times \sqrt{3}/\sqrt{2}$ (Fig. 1). We observe that each Pb atom is surrounded by three less bright protrusions forming a triangle, which are also separated by the same distance $\sim 5 \text{ \AA}$ (Fig. 1), which is nothing more than the distance between second nearest neighbors in the Ag(111) surface. It is then legitimate to assign these protrusions to Ag atoms of the first layer, even though one might then expect to observe all six Ag neighbors surrounding the Pb atom. Nevertheless, let us note that such a symmetry breaking has already been observed for the same superstructure in the case of Sb segregated on Cu(111).¹³ This is unexpected since the six Ag atoms, surrounding the Pb one in such a $(\sqrt{3} \times \sqrt{3})R30^\circ$ superstructure, are expected to be symmetry-equivalent since they all present the same geometrical environment. Nevertheless, it is known that perfectly symmetrical structures can be distorted towards less symmetric, but more stable ones in order to lower their energy by enhancing the weight of the bonding states in the local density of electronic states (Peierls-type distortion). This is observed for some bulk structures (Sb, Se, ...) but also for some surface superstructures [see, for instance, the zigzag reconstruction of (100) bcc surfaces of transition metals]. It is then tempting to interpret the contrast observed in our STM images as being due to a reconstruction of the surface layer in which three Ag neighbors of the Pb atoms “go up” whereas the three other ones “go down”. The corresponding corrugation, shown in Fig. 1, is strong but one has to keep in mind that what is measured here is the corrugation of the surface charge density which can be enhanced with respect to the atomic one.

The Pb-Ag distance being equal to that between Ag nearest neighbors ($a_{\text{Ag}}/\sqrt{2} = 2.88 \text{ \AA}$) (Fig. 1), rules out the possibility of an adsorption in ternary sites. Therefore, the only possible location for Pb atoms should be either on top adsorption as adatoms or incorporation. The latter is more consistent with the observed corrugation ($\sim 0.8 \text{ \AA}$) of Pb atoms above the Ag ones (see Table I), in view of the values of the atomic radii ($r_{\text{Ag}} = 1.45 \text{ \AA}$, $r_{\text{Pb}} = 1.75 \text{ \AA}$).

Since it is difficult to be more quantitative from the single analysis of the STM images, we then developed a detailed x ray structure analysis, using the STM information as efficient input. The x ray diffraction data consist of a set of 12 nonsymmetry-equivalent in-plane reflections and five

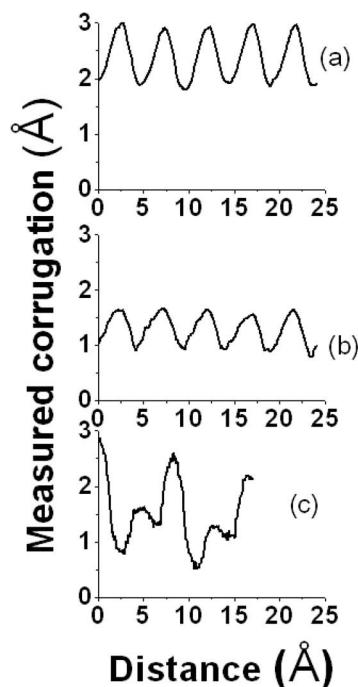
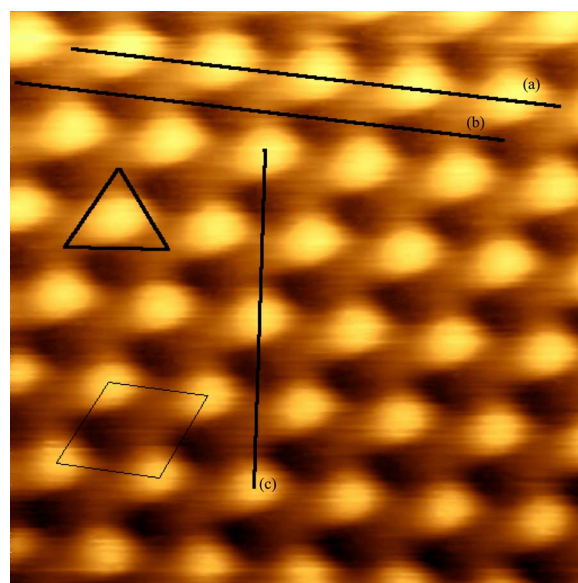


FIG. 1. (Color online) A filled state STM image at atomic resolution (2.8 nm^2 , $V = -7 \text{ mV}$, and $I = 8.25 \text{ nA}$) showing the superstructure. Line scans (a), (b), and (c) are performed along different directions indicated on the STM image. The unit cell of the superstructure is indicated by the rhombus.

nonsymmetry-equivalent rod profiles. The intensities of the in-plane reflections are shown by filled half-circles in Fig. 2. The systematic error in the data set (17 %) is estimated from the scatter of the most intense symmetry-equivalent reflections. Typical rod profiles are shown in Fig. 3.

The structural analysis is based on the comparison of experimental and calculated data from simulations of the in-plane reflections and of the rod profiles using different initial models. The standard program ROD^{14,15} is used to analyze the crystallographic data in order to determine the Pb and Ag

TABLE I. The optimum values for the atomic coordinates used to fit the experimental rod profiles. X and Y are relative coordinates ($a=0.50034$ nm, $b=0.50034$ nm). B_{\parallel} and B_{\perp} are the Debye-Waller factors. $\Delta z_{SXR D}(\text{\AA})$, and $\Delta z_{Theo}(\text{\AA})$ are the displacements of the atoms perpendicularly to the surface plane with respect to their ideal bulk positions obtained from SXR D analysis and from simulations, respectively. $\Delta z_{STM}(\text{\AA})$ is the corrugation of Pb atoms above the Ag ones deduced from the STM images.

#	X	Y	B_{\parallel}	B_{\perp}	$\Delta z_{SXR D}(\text{\AA})$	$\Delta z_{STM}(\text{\AA})$	$\Delta z_{Theo}(\text{\AA})$
Pb	0.0000	0.0000	0.90	1.10	$+0.283 \pm 0.02$	$+0.8 \pm 0.1$	+0.58
Ag ₁	0.3333	0.6666	0.63	0.78	-0.193 ± 0.02	/	-0.10
Ag ₂	0.6666	0.3333	0.63	0.78	-0.133 ± 0.02	/	-0.10

atomic coordinates. The refinement of the atomic positions in the model is performed by minimization of the usual χ^2 parameter, allowing the Debye-Waller terms (B_{\parallel} and B_{\perp}) and an appropriate scale-factor to vary. A preliminary analysis relies on the in-plane fractional order reflections, which are sensitive to the structure projected on the surface plane. The analysis of the rod profiles reveals the full three-dimensional structure.

Previous AES calibrations allow us to determine the number of Pb atoms per $p(\sqrt{3} \times \sqrt{3})R30^\circ$ unit cell, typically 1 atom, which is fully consistent with the STM images. Even though the latter seemed to indicate that the Pb atoms are inserted in the first layer, we have investigated both kinds of atomic models of the $(\sqrt{3} \times \sqrt{3})R30^\circ$ superstructure: adsorption on different sites (top, hollow, and brige sites) and substitution. A possible stacking fault of the first Ag layer has been checked also. The models with Pb adatoms are definitely ruled out since χ^2 cannot be reduced to less than three. The best fit is obtained for the model with the Pb atoms in

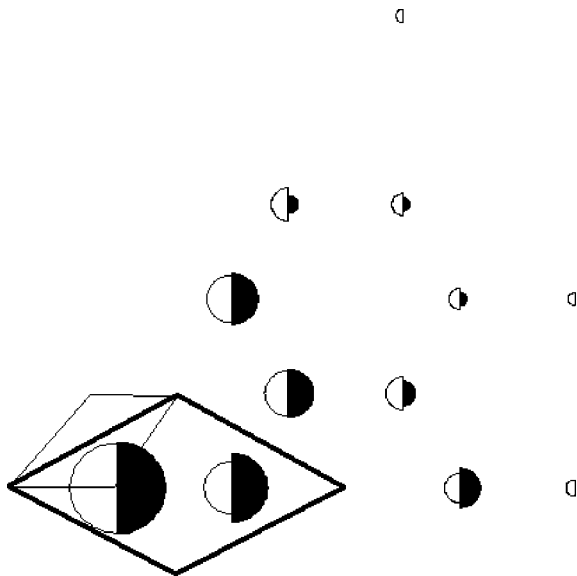


FIG. 2. The in plane SXR D intensities measured (half circle on the right) and computed (half circle on the left). The areas of the circles are proportional to the intensities. The reflections (h),(k) are indexed relative to the reciprocal unit cell of the superstructure shown by the thick rhombus. The thin rhombus represents the conventional LEED (1×1) reciprocal surface cell. The bulk Ag reflections are not represented due to their high intensities.

substitutional position in agreement with the STM indication. The final χ^2 is as small as 1.1; it is obtained after relaxing the top Ag₂Pb layer and the two first Ag underlayers (only in z -direction in order to keep the three-fold symmetry).

Figures 2 and 3 show the best fit simulations along with the experimental in-plane reflections and rod profiles. The refined model is presented in Fig. 4(a) and the atomic coordinates within the Ag₂Pb layer are given in Table I. The surface corrugation (i.e., Pb and Ag z -displacements with respect to the Ag ideal surface position), which can be seen in Fig. 4(b), is in semiquantitative agreement with the STM observations. Even though the height difference between Ag atoms ($\Delta z \sim 0.06$ Å) is smaller than that derived from the STM images, it is clearly out of the experimental error bar (see line scan “c” in Fig. 1). Both STM and SXR D experiments seem to show an “up-down” reconstruction of the Ag₂Pb layer, the magnitude of which is apparently enhanced in the STM images. However, let us remark that the appearance of the STM images can be easily caused by a tip having threefold, not circular symmetry, or by a second sub-tip that produces faint ghost images of the Pb atoms at the positions interpreted as higher Ag atoms. In addition, SXR D is not very sensitive to out of plane displacements, so it cannot really discriminate between a model with a buckling amplitude of ± 0.03 Å and a model with an unbuckled Ag layer. Therefore it is difficult to state if the buckling of the Ag layer is an artifact of the STM tip or a true distortion (possible Peierls distortion).

Nevertheless the main conclusion which is derived from the comparison of the atomically resolved STM images with the top layer arrangement deduced from the SXR D analysis [Figs. 1 and 4(a)] is clear evidence that a long range ordered 2D Ag₂Pb surface alloy has been formed.

In order to definitely confirm this ordering behavior at the surface of a phase separating system, we have calculated the adsorption and incorporation energies corresponding to the above mentioned models, which are relaxed by means of a quenched-molecular-dynamics simulation within a potential derived from the second-moment approximation (SMA) of the tight binding scheme.^{16,17,18,19} In this approximation, the energy of an atom i is written as the sum of two terms, a many body band energy derived from a simplified tight binding description of the electronic structure and a pairwise repulsive interaction of the Born-Mayer type

$$E = - \sum_i^N \sqrt{\sum_{j \neq i}^N \zeta e^{-2q[(r_{ij}/r_0)-1]}} + \sum_i^N \sum_{j \neq i}^N A e^{-p[(r_{ij}/r_0)-1]}.$$

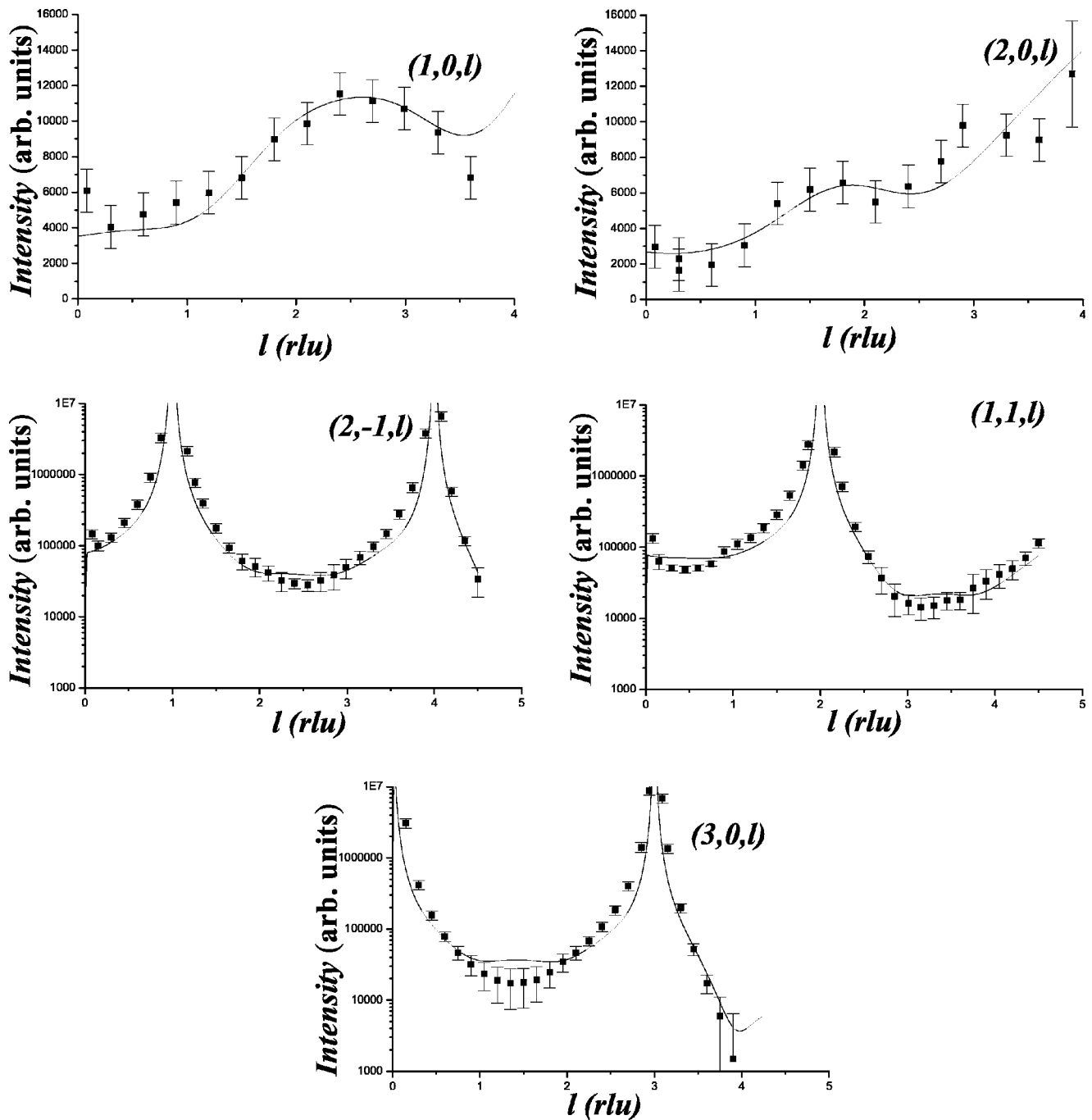


FIG. 3. The rod profiles for two nonequivalent fractional and three integer order reflections. The indices are given relative to the reciprocal unit cell of the superstructure. Data and best fit are shown by the symbols and the solid lines, respectively.

The four parameters (ζ, A, p, q) depend on the nature (Ag, Pb) of the atoms located at sites i and j [distant by r_{ij}]. When they are of the same species, they are fitted to the experimental values of the cohesive energy, the lattice parameter, and the elastic constants of the corresponding pure metals (Ag,¹⁹ Pb²⁰). For the cross terms, A and ζ are obtained from the dissolution energies of one impurity A into B and vice versa, p and q being arithmetic averages of the pure metal values. The scaling factor r_0 is chosen as the equilibrium first neighbors distance for the Ag-Ag and Pb-Pb interactions, and as their geometrical average for the Ag-Pb ones.

We fix a cut-off radius r_c for the interaction; here, r_c is taken as the second neighbor distance in Pb (larger atoms) and the potential is linked up to zero at the third neighbor distance in Ag (smaller atoms) with a fifth-order polynomial in order to avoid discontinuities both in energy and in the forces. The parameters values are given in Table II.

To determine the preferential Pb site, we have compared the adsorption/incorporation energies, after relaxation of an ordered 1/3 ML of Pb on the Ag(111) located either adsorbed in various positions (hollow, top, and bridge) or substituted inside the surface layer. The calculated energies are

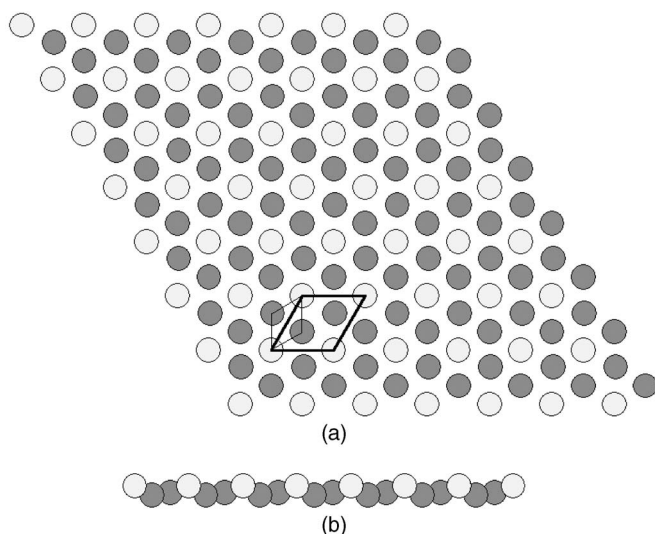


FIG. 4. A refined model of the superstructure; the atomic coordinates of the Ag_2Pb are given in Table I. (a) The top view and (b) the side view. The white circles represent the Pb atoms and the dark circles the Ag atoms.

-2.264 eV, -1.255 eV, -2.244 eV, and -2.416 eV per Pb atom respectively, showing a clear preference for the substitutional site in the surface layer. In this case, the distance between the center of Pb atom and the first Ag plane is 0.57 Å which is semiquantitative with the SXRD results ($+0.28$ Å).

Let us note that our calculation does not evidence any symmetry breaking between the six Ag atoms, contrary to experiments. This is not surprising since such Peierls-type distortions are due to modifications of the local electronic density of states which are beyond the second moment approximation used here. The modification of the energy which could result from such small atomic displacements are smaller by at least one order of magnitude than the energy balance involved in the comparison of the stabilities of the various adsorption/incorporation sites. Therefore, neglecting these distortions does not change our main conclusion, namely that substitution is preferred to adsorption.

Once again, one finds here that a 2D surface alloy can exist for a system which presents a strong chemical tendency to phase separation in the bulk. Even though the size mismatch has already been invoked to interpret similar behavior

TABLE II. The parameters of the potentials used in the molecular dynamics simulations.

#	A (eV)	ζ (eV)	p	q
Pb ²⁰	0.103	0.934	9.34	3.50
Ag ¹⁹	0.103	1.190	10.85	3.18
Ag-Pb	0.096	1.089	10.09	3.34

in a few other systems,^{21,22} the integration of “big” atoms into the surface being an efficient way to relax (at least locally) the tensile surface stress, this effect was not sufficient to reverse the tendency in the Ag/Cu(111) case.²³ More precisely, the latter theoretical study performed in both coverage limits (low and high coverages) indicates that the existence and the value of a critical coverage for such a reversal depends on surface orientation, and that it does not exist for the (111) orientation in the Ag/Cu case. The present results show that it also depends on the value of the size-mismatch, which is significantly larger here, and that such 2D ordered alloys at the surface of phase separating systems should occur whatever the orientation above a given critical size-mismatch.

IV. CONCLUSION

An atomic model derived from STM and SXRD studies is presented for the $(\sqrt{3} \times \sqrt{3})R30^\circ$ superstructure induced by $1/3$ ML Pb deposited on an Ag(111) substrate. The reconstruction consists in one Pb atom per unit cell incorporated inside the first Ag(111) plane. A quenched-molecular-dynamics study confirms that Pb atoms are indeed stabilized in substitutional sites, leading to a size-mismatch induced 2D long range ordered Ag_2Pb surface alloy.

ACKNOWLEDGEMENTS

We thank the staff of HASYLAB for their technical assistance. Financial support from the Bundesministerium für Bildung, Wissenschaft, Forschung, und Technologie (BMBF) under Project No. 05 SB8 GUA6 and the Volkswagen Stiftung is gratefully acknowledged. The work at the HASYLAB was supported in part by the European Community through the TMR program. The CRMCN is associated with the Universities of Aix-Marseille II and III.

*Author to whom correspondence should be addressed. FAX: +33 4 91 82 91 97. Electronic address: Hamid@crmcn.univ-mrs.fr

¹U. Bardi, Rep. Prog. Phys. **57**, 939 (1994).

²P. Wynblatt and R. C. Ku, Surf. Sci. **65**, 511 (1977).

³B. Legrand, A. Saúl, and G. Tréglia, *Materials Science Forum* (Trans Tech Publi, Switz), 155-156, 165 (1994). See also: G. Tréglia, A. Saúl, and B. Legrand, *Il Vuoto, Scienza e Tecnologia*, (1996) Vol. XXV N4.

⁴A. Christensen, A. V. Ruban, P. Stoltze, K. W. Jacobsen, H. L. Skriver, J. K. Nørskov, and F. Besenbacher, Phys. Rev. B **56**,

5822 (1997).

⁵See the contributions involved in the book *Modelling and Simulation of Surface Segregation in Alloys*, Computational Materials Science 15 (1999).

⁶J. Eugène, B. Aufray, and F. Cabané, Surf. Sci. **241**, 1 (1991).

⁷Y. Liu and P. Wynblatt, Surf. Sci. **240**, 245 (1990).

⁸H. Giordano, O. Alem, and B. Aufray, Scr. Metall. Mater. **28**, 257 (1993).

⁹K. Takayanagi, D. M. Kolb, K. Kambe, and G. Lehmppuhl, Surf. Sci. **100**, 407 (1980).

- ¹⁰A. Rolland, J. Bernardini, and M. G. Barthes-Labrousse, *Surf. Sci.* **143**, 579 (1984).
- ¹¹G. Wittich, L. Vitali, M. A. Schneider, and K. Kern (Extended Abstract presented at ECOSS-22, Prague, 2003).
- ¹²R. Widmer and H. Siegenthaler, *J. Electrochem. Soc.* **151**, 238 (2004).
- ¹³B. Aufray, H. Giordano, and D. N. Seidman, *Surf. Sci.* **447**, 180 (2000).
- ¹⁴E. Vlieg, A. W. Denier Van Der Gon, J. F. Van Der Veen, J. E. MacDonald, and C. Norris, *Surf. Sci.* **209**, 100 (1989).
- ¹⁵E. Vlieg, *J. Appl. Crystallogr.* **33**, 401 (2000).
- ¹⁶V. Rosato, M. Guillopé, and B. Legrand, *Philos. Mag. A* **59**, 321 (1989).
- ¹⁷L. Verlet, *Phys. Rev.* **159**, 98 (1967).
- ¹⁸C. H. Bennett, in *Diffusion in Solids, Recent Developments*, edited by Nowick and Burton (Academic, New York, 1975), p.73.
- ¹⁹C. Mottet, G. Tréglia, and B. Legrand, *Phys. Rev. B* **46**, 16018 (1992).
- ²⁰F. Cléri and V. Rosato, *Phys. Rev. B* **48**, 22 (1993).
- ²¹J. Tersoff, *Phys. Rev. Lett.* **74**, 434 (1995) and references therein.
- ²²C. Nagl, E. Platzgummer, M. Schmid, P. Varga, S. Speller, and W. Heiland, *Surf. Sci.* **352–354**, 540 (1996).
- ²³I. Meunier, G. Tréglia, and B. Legrand, *Surf. Sci.* **441**, 225 (1999).